Title page

Title

Fully Automatic Software for Detecting Radiographic Joint Space Narrowing Progression in Rheumatoid Arthritis: Phantom Study and Comparison with Visual Assessment

Taichi Okino, RT, MS[1,2], Yafei Ou[3], Masayuki Ikebe, PhD[4], Kenichi Tamura, PhD[5], Kenneth Sutherland, PhD[6], Jun Fukae, MD, PhD[7], Kazuhide Tanimura, MD[8], Tamotsu Kamishima, MD, PhD[9]

1 Department of Radiological Technology, Sapporo City General Hospital
North-11 West-13, Chuo-ku, Sapporo, 060-8604, Japan
E-mail: taichi.okino@frontier.hokudai.ac.jp

2 Graduate School of Health Sciences, Hokkaido University
North-12 West-5, Kita-ku, Sapporo, 060-0812, Japan
E-mail: taichi.okino@frontier.hokudai.ac.jp

3 Research Center for Integrated Quantum Electronics, Hokkaido University
North-13, West-8, Kita-ku, Sapporo, 060-8628, Japan
E-mail: yafei.ou.x5@elms.hokudai.ac.jp

4 Research Center for Integrated Quantum Electronics, Hokkaido University
North-13, West-8, Kita-ku, Sapporo, 060-8628, Japan
E-mail: ikebe@ist.hokudai.ac.jp

5 Department of Mechanical Engineering, College of Engineering, Nihon University
Nakagawara-1, Tokusada, Tamuramachi, Koriyama, Fukushima, 963-8642, Japan
E-mail: tamura.kennichi@nihon-u.ac.jp

6 Global Center for Biomedical Science and Engineering, Hokkaido University
North-15 West-7, Kita-ku, Sapporo 060-8638, Japan
E-mail: kensuth@med.hokudai.ac.jp

7 (Previous) Hokkaido Medical Center for Rheumatic Diseases

1-45 3-Chome, 1-Jo, Kotoni, Nishi-ku, Sapporo, 063-0811, Japan
E-mail: jun.fukae@ryumachi-jp.com
(Current) Kuriyama Red Cross Hospital
3-2, Asahi, Kuriyama-cyo, Yubari-gun, Hokkaido, 069-1513, Japan
e-mail: jun.fukae@ryumachi-jp.com

8 Hokkaido Medical Center for Rheumatic Diseases
1-45 3-Chome, 1-Jo, Kotoni, Nishi-ku, Sapporo, 063-0811, Japan
E-mail: k.tanimura@pep.ne.jp

9 Faculty of Health Sciences, Hokkaido University
North-12 West-5, Kita-ku, Sapporo, 060-0812, Japan
E-mail: ktamotamo2@hs.hokudai.ac.jp

Address correspondence to:
Tamotsu Kamishima, MD, PhD,
Faculty of Health Sciences, Hokkaido University
North-12, West-5, Kita-ku, Sapporo 060-0812, Japan
Phone; 81-11-706-2824
E-mail; ktamotamo2@hs.hokudai.ac.jp
http://www.hs.hokudai.ac.jp/kamishima/index.html

Type of manuscript: Original article

Declarations

Ethics approval and consent to participate

All procedures performed in studies involving human participants were in accordance with the ethical standards of the institutional research committee and with the 1964 Helsinki Declaration.

Informed consent

Informed consent was obtained from all patients.

Conflict of interest

The authors declare that they have no conflict of interest.

Acknowledgements
We sincerely appreciate Ms. Yuko Aoki, Ms. Mihoko Henmi, and Mr. Fumihiko Sakamoto for their technical assistant in terms of image acquisition.

Word count of the text (not including references): 3553

secondary abstract (50 words)

We have developed and validated the in-house software with partial image phase-only correlation (PIPOC) in terms of detecting slight radiographic finger joint space narrowing (JSN) progressions with rheumatoid arthritis patients using the Genant-modified Sharp score and the power Doppler ultrasonography assessments as well as in phantom finger JSN assessment.
-

Fully Automatic Software for Detecting Radiographic Joint Space Narrowing Progression in Rheumatoid Arthritis: Phantom Study and Comparison with Visual Assessment

Abstract

Purpose We have developed an in-house software equipped with partial image phase-only correlation (PIPOC) which can automatically quantify radiographic joint space narrowing (JSN) progression. The purpose of this study was to evaluate the software in phantom and clinical assessments.

Materials and methods In the phantom assessment, the software's performance on radiographic images was compared to the joint space width (JSW) difference using a micrometer as ground truth. A phantom simulating a finger joint was scanned underwater. In the clinical assessment, 15 RA patients were included. The software measured the radiological progression of the finger joints between baseline and the 52nd week. The cases were also evaluated with the Genant-modified Sharp score (GSS), a conventional visual scoring method. We also quantitatively assessed these joints' synovial vascularity (SV) on PDUS (0, 8, 20, and 52 weeks).

Results In the phantom assessment, the PIPOC software could detect changes in JSN with a smallest detectable difference of 0.044 mm at 0.1 mm intervals. In the clinical assessment, the JSW change of the joints with GSS progression detected by the software was significantly greater than those without GSS progression ($p = 0.004$). The JSW change of joints with positive SV at baseline was significantly higher than those with

negative SV ($p = 0.024$).

Conclusion Our in-house software equipped with PIPOC can automatically and quantitatively detect slight radiographic changes of JSW in clinically inactive RA patients.

Keywords:

Connective tissue disease; Radiography; Joint destruction; Software; Ultrasonography

Introduction

Rheumatoid arthritis (RA) is characterized by synovial inflammation and bone destruction leading to disability with potential large socioeconomic consequences for the individual patient and society [1]. The emphasis is now on early intervention to prevent disability and irreversible damage. Early detection and diagnosis of RA are extremely important to avoid missing the "window of opportunity" to start effective therapeutic agents, resulting in long-term sustained benefits or, more importantly, the chance of "cure" [2].

Radiography has been the primary imaging modality for the evaluation of structural joint damage both in clinical practice and clinical trials. The advantages of radiography for RA include excellent skeletal structure imaging and comprehensive assessment of joints, as well as low cost and general accessibility [3, 4]. The gold standard to assess radiographic joint destruction in RA is the semi-quantitative van der Heijde-modified Sharp score or the Genant-modified Sharp score (GSS), in which radiologists and rheumatologists visually assess the progression of joint space narrowing (JSN) and bone erosion [5-7]. As Kato et al. reported, even for experienced rheumatologists in GSS assessment, it is difficult to detect joint space width (JSW) difference of 0.30 mm or less [8], making it extremely challenging to detect slight changes visually.

In the last two decades, a trend toward lower levels in disease activity, and hence in radiographic progression among the cohort of patients receiving methotrexate has been noted in trials [9], hypothesized to be due to a better standard of care for RA patients. Even with the availability of high-resolution imaging, it is not uncommon for JSN progression to be less than a few pixels per year; a high level of accuracy and precision is therefore required to detect slight progression in clinical trials [10].

Several computer-based software methods have been developed and introduced [11-14]; however, most use traditional image processing and machine learning methods to detect the bone margin and then calculate JSW. Because of the two-dimensional nature of the radiograph, it is difficult to improve the accuracy of the bone margin. Algorithms based on margins have pixel-level errors, and it is theoretically almost impossible to detect early JSW changes that are less than one pixel in early-stage RA patients.

We, therefore, have developed in-house software equipped with partial image phase-only correlation (PIPOC) which can automatically calculate the displacements of multiple areas with sub-pixel accuracy. To validate the software, we conducted a phantom assessment. We then assessed JSN progression by the GSS and synovial vascularity (SV) by quantitative power Doppler ultrasonography (PDUS). The purpose of this study was to evaluate the in-house software with PIPOC in terms of detecting slight radiographic

progression in finger JSN using the GSS and the PDUS assessments as well as in phantom finger JSN.

Material and methods

Phantom assessment

A phantom finger joint in a water tank was imaged by radiography. The JSW was changed at intervals of 0.1 and 0.01 mm. The delta (Δ) JSWs, or changes from JSN = 1.2 and 1.65 mm for 0.1 mm and 0.01 mm intervals, respectively, were used to evaluate the process of JSN by the PIPOC method.

Phantom

A metacarpophalangeal joint-shaped two-layer (subchondral bone and cancellous bone) phantom with a water tank (Fig. 1) was used in the experiment. The phantom was made of titanium medical apatite (TMA) [15]. TMA is a recently introduced material that is easier to model than hydroxyapatite, and its CT value (Hounsfield units) is equivalent to that of subchondral and cancellous bones. The phantom mimics the metacarpophalangeal joint, and the JSW can be freely changed at 0.01 mm intervals. The composition of the

phantom is shown in Table 1.

Imaging with radiography

The phantom's joint center was used as the imaging center. Imaging was performed using radiography where the attached water tank was full of water. Digital radiographs were acquired with CALNEO smart C47 (Fujifilm, Tokyo, Japan) under the following conditions: tube voltage = 50 kV; tube current = 100 mA; exposure time = 0.02 sec; source to detector distance = 100 cm; pixel size = 0.15 mm. Also, referring to the average JSW of women within the RA prevalence age, the phantom JSW was changed at intervals of 0.1 mm between 1.2 and 2.2 mm and at intervals of 0.01 mm between 1.65 and 1.75 mm in water. In total, 21 measurements were taken.

In-house software equipped with PIPOC

We have developed in-house software equipped with PIPOC. The PIPOC method is an improvement over the full image phase-only correlation (FIPOC) method proposed by Ou et al. [16, 17]. The FIPOC is an approach to estimating the relative translative offset between two similar images that relies on analyzing images in the frequency domain. The analysis procedure was performed following five steps (Fig. 2).

1. Positioning fingers

Initially, the background of radiographic images is subtracted using Otsu's method [18]. The morphological opening and closing are used to remove small objects and holes. Next, we find grooves and fingertips by the edge of the hand. Then, we calculate the area of the finger and fit a line through the center of this area. Last, we calculate the width of the fingers by the size of the finger area. Therefore, the finger area can be cut out to detect the position of the joint.

2. Joint detection

The next step is the detection of the joints. We use AdaBoost's machine learning algorithm to train our joint classifier [19].

3. Position Calibration

As shown in step 3 of Fig. 2, the cyan and red lines are the bone edges of the baseline and follow-up images, respectively. The white line represents coincidental parts. Before position calibration, detection results of the same joint in sequential radiographic images have a deviation in the position of joint windows. We use the FIPOC to calibrate the position of the joint. The deviation between the two joint windows can be mostly eliminated when their edges are almost completely coincident.

4. Joint segmentation

We propose an algorithm to segment joint images so that the movement of the proximal and distal bones can be detected separately. To avoid mutual interference, a dividing line is drawn in the gully to calculate the movement of the proximal and distal bones separately.

5. Joint Comparison

As shown in step 5 of Fig. 2, PIPOC is used to calculate the relative movement of the proximal and distal bones. Each joint image is divided into proximal and distal bones in the phase spectrum in this step. We then calculate the phase difference spectrum of proximal and distal bones between the baseline and follow-up images. The bone movement can be obtained by calculating the peak position of the Dirac delta function in the phase difference spectrum. Thus, the JSN between the baseline and follow-up images can be quantified according to the bone movement difference between proximal and distal bones. A median filter is used to suppress the noise before calibrating the minute displacement using PIPOC. From these steps, we can calculate the progression of JSN according to the vertical movements of the proximal and distal bones. We describe the details of the PIPOC algorithm in a previous study [20].

Clinical assessment

Patients

Fifteen patients meeting the 1987 American College of Rheumatology classification

criteria for RA [21] and long-term sustained clinical low disease activity (CLDA) were analyzed retrospectively. The patients had been treated with non-biologic disease-modifying antirheumatic drugs (DMARDs) (eight patients with methotrexate [MTX], three patients with MTX + tacrolimus) or with biologics (one patient with MTX + adalimumab, two patients with MTX + tocilizumab [TCZ] and one patient with TCZ monotherapy). The clinical and laboratory characteristics of the patients are presented in Table 2. This study was conducted in accordance with the Declaration of Helsinki. The local ethics committee approved the study, and informed consent was obtained from all patients.

Ultrasonography

All patients underwent 3D PDUS of metacarpophalangeal (MCP) and proximal interphalangeal (PIP) joints over the dorsal surface in the longitudinal plane at baseline and weeks 8, 20, and 52 by one of three US experts specialized in musculoskeletal ultrasonography who were blinded to other clinical information. A linear array transducer (13 MHz) and US equipment were used (EUP-L34P, HI VISION Avius; Hitachi, Tokyo, Japan). The details of the PDUS settings and the quantitative PDUS method were described in a previous study [22-25]. Using quantitative PDUS, the SV value was

determined by counting the number of vascular flow pixels in the region of interest (ROI).

Radiography

Plain radiographs of the hands at baseline and at the 52nd week for all patients using Radnext 32 (Hitachi, Tokyo, Japan) under the following conditions: tube voltage = 50 kV; tube current = 100 mA; exposure time = 0.025 sec; source to detector distance = 100 cm; pixel size = 0.15 mm. All radiographs were scored by an expert rheumatologist with more than 15 years of experience who was blinded to other clinical information for assessment of JSN progression using the GSS system as follows: 0 = normal; 0.5 = subtle or equivocal narrowing; 1.0 = focal or mild narrowing; 1.5 = mild-to-moderate narrowing; 2.0 = moderate narrowing; 2.5 = moderate-to-severe narrowing; 3.0 = complete loss of joint space or dislocation in the presence of erosion; 3.5 = partial or equivocal ankylosis; 4.0 = definite ankylosis [6, 26]. The intra-observer reliability of the GSS method for this study population has already been shown in previous studies [8, 27].

Statistical analysis

Statistical analyses were performed with the use of Microsoft Excel 2019 (Microsoft,

Redmond, WA, USA) and EZR software version 1.40 (Saitama Medical Center, Jichi Medical University, Saitama, Japan) [28], which is a graphical user interface for R software package version 3.5.2 (The R Foundation for Statistical Computing, Vienna, Austria). A p-value < 0.05 was considered to indicate a significant difference.

In the phantom assessment, the mean error and the standard deviation (SD) of the differences between theoretically true JSW derived from the measurement via the micrometer and measured JSW were calculated as an index to evaluate the random error. The smallest detectable difference (SDD) represents the smallest difference between two independently obtained measures which can be distinguished from measurement error. The SDD for measured JSW was calculated according to the following formula:

$$\mathrm{SDD} = 1.96 \times \mathrm{SD}_{\mathrm{diff}}$$

where $\mathrm{SD}_{\mathrm{diff}}$ was the SD of the difference between theoretical and measured JSW [29-31]. A linear regression test validated the relationships between the theoretically true JSW and the measured JSW differences.

In the clinical assessment, quantitative variables were given as median and interquartile range (IQR) or mean and SD. Differences in parameters were examined using the Mann–Whitney U test. We compared the JSW (mm) calculated by in-house software between the progressive and non-progressive finger joints according to the

ΔGSS. The interval score difference of the GSS between baseline and follow-up was compared to confirm that the in-house software can detect interval JSN progression in the visual assessment results. We then compared the ΔGSS and the JSW in the positive and negative SV finger joints in the ultrasonographic findings at baseline. Joints with positive SV at baseline [b-SV (+)] were defined as those with positive SV detected in the ROI at baseline. In contrast, joints without SV signals during the follow-up period were defined as negative SV [SV (-)]. This analysis demonstrated that finger joints with positive SV at baseline cause structural destruction in RA.

The sum-SV value, the total value of SV signals, was calculated for joints with positive SV during the follow-up period. To ascertain whether structural destruction depends on synovial blood flow inflammation, we divided the positive SV joints into sum-SV high and low groups by the median value and examined differences in JSN progression.

Results

Phantom assessment

The mean error, SD and SDD for JSW measurements at 0.1 mm and at 0.01 mm intervals

are shown in Table 3. The correlations between true JSW and measured JSW differences are shown in Fig. 3. There were significant correlations between true JSW and measured JSW differences ranging from 1.2 to 2.2 mm at 0.1 mm intervals ($R^2 = 0.996$; $p < 0.001$), and from 1.65 to 1.75 mm at 0.01 mm intervals ($R^2 = 0.553$; $p = 0.009$).

Clinical assessment

We analyzed the 1st to 5th MCP joints and the 2nd to 5th PIP joints in 15 RA patients. Out of 270 joints, we targeted 261 finger joints after excluding nine damaged joints (ankylosis, complete luxation, and subluxation). The success rate of the in-house software JSW analysis was 99.6% (260/261). The software analysis failed to locate one joint. Subsequent analyses were therefore performed for the remaining 260 joints.

Images of 260 joints in 15 patients regarding GSS, JSW, and SV of the finger joints were scored or measured. The medians of GSS at baseline, at follow-up and the ΔGSS were 1 (IQR 1-2, n; the number of joints = 260), 1 (IQR 1-2, n = 260) and 0 (IQR 0-0, n =260), respectively. Out of 260 joints, ΔGSS (+) was assigned to joints with positive ΔGSS according to the GSS results (n = 37, 14.23%). Otherwise, ΔGSS (-) was assigned to the others (n = 223, 85.77%). The median of JSW was 0.001 mm (IQR -0.491 mm – 0.496 mm, n = 260). The medians of SV at baseline, the 8th week, the 20th week,

and the 52nd week were the same values (0 [IQR 0-0, n = 260]). The number of joints with baseline positive and negative SV were 32 and 211, respectively.

The JSW of the finger joints with GSS progression [ΔGSS (+)] detected by the in-house software was significantly greater than those without GSS progression [ΔGSS (-)] (Mann-Whitney U test, p = 0.004). The median JSW of ΔGSS (-) and ΔGSS (+) were 0.029 mm (IQR -0.434 mm – 0.496 mm, n = 223) and -0.443 mm (IQR -1.434 mm – -0.102 mm, n = 37), respectively (Fig. 4).

The ΔGSS of finger joints with positive SV at baseline [b-SV (+)] were significantly higher than those with negative SV [SV (-)] ($p < 0.001$) (Fig. 5a). The JSW of finger joints with positive SV at baseline [b-SV (+)] was significantly higher than those with negative SV [SV (-)] (p = 0.024) (Fig. 5b).

We calculated the sum-SV value by summation of the sequential SV value of each joint. The median of the sum-SV value was 147 pixels (IQR 49-367.5, n = 32). The median ΔGSS of the high group and the low group of the sum-SV were 0.25 (IQR 0 – 0.5, n = 16) and 0 (IQR 0 – 0.125, n = 16), respectively. The median JSW of the high group and the low group of the sum-SV were -0.350 mm (IQR -1.026 mm – 0.383 mm, n = 16) and -0.636 mm (IQR -1.140 mm – 0.096 mm, n = 16), respectively. There were no significant differences between the high and low group of sum-SV joints with both

analyses using the GSS and the in-house software ($p = 0.192$ and $p = 0.926$) (Fig. 6). In joints with positive SV, changes in JSN progression did not relate to the sum-SV.

Discussion

In this study, our in-house software equipped with PIPOC could automatically and quantitatively detect slight JSN progression. The results were comparable to conventional scoring methods. The present study is novel in that it applies the PIPOC technique to joint detection and directly compares the software and the doctor's visual assessment based on ultrasound findings.

Several groups have researched JSW quantification using software with clinical practice cases and have achieved promising results [32, 33]. Huo et al. performed JSW quantification in early RA patients using the automated JSW quantification software 'JSQ' [32]. Comparing the SHS method with the software evaluation, a similar trend was seen with the yearly progression rate of JSW change. However, they reported that the software might fail to detect JSW in some cases, such as when joint edges overlap or the distal bone margin cannot be identified.

A computer-based method named joint space difference index (JSDI) has been

developed and examined, which can semi-automatically calculate an index showing the degree of JSN progression [27, 34]. The software was designed to avoid distal bone margin problems by utilizing a method of superimposing two images between baseline and follow-up. However, the software using JSDI had some drawbacks. Since the JSDI calculated the difference in pixel values, it is strongly affected by image density and acquisition conditions. In addition, the superimposition of two images and the region's setting of interest were done manually and could not be fully automated. Kato et al. modified this software to enable the automatic calculation of JSDI [35]. The JSDI displays the absolute value of the change in JSW between two images, so it remains a drawback that it cannot identify whether the JSW was widening or narrowing.

To address these issues, we tried a completely new approach. The phase-only correlation (POC) method is superior in robustness and positional accuracy. In high-precision image matching with POC, the displacement of an image can be estimated with an accuracy of 1/10 to 1/100 pixel by a function fitting technique using the closed-form representation of the POC function's peak [36]. We have developed an in-house software equipped with PIPOC, which can automatically calculate the displacements of multiple areas with sub-pixel accuracy. We, therefore, used an underwater phantom to confirm the performance of the fundamental software and performed a clinical assessment to

determine how close the software could come to conventional scoring methods.

In the phantom assessment, the mean error and SDD underwater at 0.1 mm intervals were 0.001 mm and 0.044 mm, respectively. We also found significant correlations between true JSW and measured JSW differences in all measurement conditions. A similar phantom experiment was executed by Huétink et al., who studied the systematic error and sensitivity (defined as the SDD) of the computerized JSW measurements in an acrylic phantom joint and human cadaver-derived phalangeal joints both surrounded by the air [37]. The mean systematic error and SDD in an acrylic phantom/human cadaver phantom were 0.054 mm and 0.037 mm / 0.210 mm and 0.226 mm, respectively. Our software can perform JSW analysis with an order of magnitude finer accuracy than previous phantom studies, despite the more unfavorable underwater condition. Furthermore, the TMA phantoms were made to mimic human bones in terms of shape and CT values, which enables us to examine the structure of the real human anatomy more closely than simple acrylic phantoms.

In the clinical assessment, our in-house software compared to the GSS in radiographic JSN progressions was consistent with the conventional scoring method. The software and the doctor's visual assessment showed that the joints with positive SV at baseline were associated with JSN progression. However, in the positive SV joints, there

was no significant difference in JSN progression depending on the total value of the signal. This means that the joint with positive SV at baseline, i.e., synovial inflammation joints in the early stages of RA, will have progressive subsequent bone destruction, regardless of its degree of inflammation. Fukae et al. reported in joints with smoldering inflammation, structural damage progresses independently of the level of synovial vascular summation [24]. It is, therefore, clinically meaningful that the software can detect a slight JSN progression in patients with CLDA.

In clinical trials of patients with RA, it has become increasingly difficult for conventional radiographic scoring systems to detect statistically significant changes in joint deterioration. This is attributed to early escape study designs and the shorter duration of treatment in the placebo group, which leads to a lower radiographic progression rate [33, 39]. In contrast, hand radiographs' computer-based methods seem more sensitive to detecting subtle changes in progressive JSN [8, 27, 35]. Fully automatic software, such as the one we have developed here, enables early disease detection and helps physicians with extensive routine reading tasks. Using such effective tools is also expected to reduce the burden of health care costs [40]. In addition, we are working on further refinement of the software to make it applicable to the MCP/PIP joints and the other joints, such as the carpal bones.

There are several limitations to this study. First, the clinical assessment was conducted retrospectively. There is a risk that the radiographs may not be optimal for the software analysis, e.g., the difference in the finger angle between baseline and follow-up. In contrast, it is meaningful to test our software on the images acquired in a real clinical setting, even if the images are unsuitable for software analysis. Second, the sample size was small and limited to a single hospital. We need to confirm our observations with a large-scale population in multiple institutions. Third, the software analysis is quite accurate in JSW measurements but not perfect. Certain joint structures and positioning might result in incorrect edge detection; this might be a factor that reduces the accuracy of the results in JSW measurements. Schenk et al. reported that the failure of computerized JSW analysis was more frequently caused by technical factors during image acquisition, such as differences between baseline and follow-up hand positioning, than by the automatic analysis system [38]. Therefore, it is important to standardize the imaging technique and further improve the software for commercialization in clinical practice.

In conclusion, our in-house software equipped with PIPOC can automatically and quantitatively detect slight radiographic changes of JSW in RA patients with CLDA. The clinical results in this study were confirmed using a specially designed phantom

underwater, although further evaluation and refinement are needed.

References

1. Scott DL, Wolfe F, Huizinga TW. Rheumatoid arthritis. The Lancet. 2010;376:1094-108.
2. Quinn M, Emery P. Window of opportunity in early rheumatoid arthritis: possibility of altering the disease process with early intervention. Clinical and experimental rheumatology. 2003;21:S154-S7.
3. Ornbjerg LM, Ostergaard M. Assessment of structural damage progression in established rheumatoid arthritis by conventional radiography, computed tomography, and magnetic resonance imaging. Best Pract Res Clin Rheumatol. 2019;33:101481.
4. Van der Heijde D. Radiographic imaging: the'gold standard'for assessment of disease progression in rheumatoid arthritis. Rheumatology (Oxford, England). 2000;39:9-16.
5. Van der Heijde D. How to read radiographs according to the Sharp/van der Heijde method. The Journal of rheumatology. 2000;27:261-3.
6. Genant HK, Jiang Y, Peterfy C, Lu Y, Rédei J, Countryman PJ. Assessment of rheumatoid arthritis using a modified scoring method on digitized and original radiographs. Arthritis & Rheumatism: Official Journal of the American College of Rheumatology. 1998;41:1583-90.
7. Ravindran V, Rachapalli S. An overview of commonly used radiographic scoring methods in rheumatoid arthritis clinical trials. Clin Rheumatol. 2011;30:1-6.
8. Kato K, Yasojima N, Tamura K, Ichikawa S, Sutherland K, Kato M, et al. Detection of Fine Radiographic Progression in Finger Joint Space Narrowing Beyond Human Eyes: Phantom Experiment and Clinical Study with Rheumatoid Arthritis Patients. Sci Rep. 2019;9:8526.
9. Rahman MU, Buchanan J, Doyle MK, Hsia EC, Gathany T, Parasuraman S, et al. Changes in patient characteristics in anti-tumour necrosis factor clinical trials for rheumatoid arthritis: results of an analysis of the literature over the past 16 years. Ann Rheum Dis. 2011;70:1631-40.
10. Shimizu T, Cruz A, Tanaka M, Mamoto K, Pedoia V, Burghardt AJ, et al. Structural

Changes over a Short Period Are Associated with Functional Assessments in Rheumatoid Arthritis. J Rheumatol. 2019;46:676-84.

11. Duryea J, Jiang Y, Zakharevich M, Genant HK. Neural network based algorithm to quantify joint space width in joints of the hand for arthritis assessment. Med Phys. 2000;27:1185-94.
12. Langs G, Peloschek P, Bischof H, Kainberger F. Automatic quantification of joint space narrowing and erosions in rheumatoid arthritis. IEEE Trans Med Imaging. 2009;28:151-64.
13. Pfeil A, Oelzner P, Bornholdt K, Hansch A, Lehmann G, Renz DM, et al. Joint damage in rheumatoid arthritis: assessment of a new scoring method. Arthritis Research & Therapy. 2013;15:R27.
14. Huo Y, Vincken KL, van der Heijde D, De Hair MJ, Lafeber FP, Viergever MA. Automatic Quantification of Radiographic Finger Joint Space Width of Patients With Early Rheumatoid Arthritis. IEEE Trans Biomed Eng. 2016;63:2177-86.
15. Tamura K. Mechanical Properties of a Vacuum-Sintered Apatite Body for Use as Artificial Bone. Journal of Biomaterials and Nanobiotechnology. 2015;06:45-52.
16. Ou Y, Ambalathankandy P, Shimada T, Kamishima T, Ikebe M. Automatic Radiographic Quantification of Joint Space Narrowing Progression in Rheumatoid Arthritis Using POC. 2019 IEEE 16th International Symposium on Biomedical Imaging (ISBI 2019). 2019:1183-7.
17. Taguchi A, Shishido S, Ou Y, Ikebe M, Zeng T, Fang W, et al. Quantification of Joint Space Width Difference on Radiography Via Phase-Only Correlation (POC) Analysis: a Phantom Study Comparing with Various Tomographical Modalities Using Conventional Margin-Contouring. J Digit Imaging. 2021;34:96-104.
18. Otsu N. A threshold selection method from gray-level histograms. IEEE transactions on systems, man, and cybernetics. 1979;9:62-6.
19. Viola P, Jones M. Rapid object detection using a boosted cascade of simple features. Proceedings of the 2001 IEEE computer society conference on computer vision and pattern recognition CVPR 2001. 2001;1:I-I.
20. Ou Y, Ambalathankandy P, Furuya R, Kawada S, Zeng T, An Y, et al. A Sub-pixel Accurate Quantification of Joint Space Narrowing Progression in Rheumatoid Arthritis. arXiv preprint arXiv:220509315. 2022.
21. Arnett FC, Edworthy SM, Bloch DA, McShane DJ, Fries JF, Cooper NS, et al. The American Rheumatism Association 1987 revised criteria for the classification of rheumatoid arthritis. Arthritis Rheum. 1988;31:315-24.
22. Fukae J, Kon Y, Henmi M, Sakamoto F, Narita A, Shimizu M, et al. Change of synovial

vascularity in a single finger joint assessed by power doppler sonography correlated with radiographic change in rheumatoid arthritis: Comparative study of a novel quantitative score with a semi-quantitative score. Arthritis Care & Research. 2010;62:657-63.

23. Fukae J, Isobe M, Kitano A, Henmi M, Sakamoto F, Narita A, et al. Radiographic prognosis of finger joint damage predicted by early alteration in synovial vascularity in patients with rheumatoid arthritis: Potential utility of power doppler sonography in clinical practice. Arthritis Care Res (Hoboken). 2011;63:1247-53.
24. Fukae J, Isobe M, Kitano A, Henmi M, Sakamoto F, Narita A, et al. Positive synovial vascularity in patients with low disease activity indicates smouldering inflammation leading to joint damage in rheumatoid arthritis: time-integrated joint inflammation estimated by synovial vascularity in each finger joint. Rheumatology (Oxford). 2013;52:523-8.
25. Fukae J, Isobe M, Kitano A, Henmi M, Sakamoto F, Narita A, et al. Structural deterioration of finger joints with ultrasonographic synovitis in rheumatoid arthritis patients with clinical low disease activity. Rheumatology (Oxford). 2014;53:1608-12.
26. Peterfy CG, Wu C, Szechinski J, DiCarlo JC, Lu Y, Genovese M, et al. Comparison of the Genant-modified Sharp and van der Heijde-modified Sharp scoring methods for radiographic assessment in rheumatoid arthritis. International Journal of Clinical Rheumatology. 2011;6:15-24.
27. Okino T, Kamishima T, Lee Sutherland K, Fukae J, Narita A, Ichikawa S, et al. Radiographic temporal subtraction analysis can detect finger joint space narrowing progression in rheumatoid arthritis with clinical low disease activity. Acta Radiol. 2018;59:460-7.
28. Kanda Y. Investigation of the freely available easy-to-use software 'EZR' for medical statistics. Bone Marrow Transplant. 2013;48:452-8.
29. Bland JM, Altman D. Statistical methods for assessing agreement between two methods of clinical measurement. The lancet. 1986;327:307-10.
30. Ejbjerg BJ, Vestergaard A, Jacobsen S, Thomsen HS, Ostergaard M. The smallest detectable difference and sensitivity to change of magnetic resonance imaging and radiographic scoring of structural joint damage in rheumatoid arthritis finger, wrist, and toe joints: a comparison of the OMERACT rheumatoid arthritis magnetic resonance imaging score applied to different joint combinations and the Sharp/van der Heijde radiographic score. Arthritis Rheum. 2005;52:2300-6.
31. Bruynesteyn K, Boers M, Kostense P, van der Linden S, van der Heijde D. Deciding on progression of joint damage in paired films of individual patients: smallest detectable difference or change. Ann Rheum Dis. 2005;64:179-82.

32. Huo Y, Veldhuizen R, van der Heijde D, Besselink N, Jacobs J, van Laar J, et al. Automated joint space width quantification of hand and wrist joints: a proof of concept study. Clin Exp Rheumatol. 2016;34:S34-S9.
33. Pfeil A, Nussbaum A, Renz DM, Hoffmann T, Malich A, Franz M, et al. Radiographic remission in rheumatoid arthritis quantified by computer-aided joint space analysis (CASJA): a post hoc analysis of the RAPID 1 trial. Arthritis Res Ther. 2020;22:229.
34. Ichikawa S, Kamishima T, Sutherland K, Okubo T, Katayama K. Radiographic quantifications of joint space narrowing progression by computer-based approach using temporal subtraction in rheumatoid wrist. Br J Radiol. 2016;89:20150403.
35. Kato K, Sutherland K, Tanaka Y, Kato M, Fukae J, Tanimura K, et al. Fully automatic quantitative software for assessment of minute finger joint space narrowing progression on radiographs: evaluation in rheumatoid arthritis patients with long-term sustained clinical low disease activity. Jpn J Radiol. 2020;38:979-86.
36. Nagashima S, Aoki T, Higuchi T, Kobayashi K. A subpixel image matching technique using phase-only correlation. 2006 International Symposium on Intelligent Signal Processing and Communications. 2006:701-4.
37. Huetink K, van 't Klooster R, Kaptein BL, Watt I, Kloppenburg M, Nelissen RG, et al. Automatic radiographic quantification of hand osteoarthritis; accuracy and sensitivity to change in joint space width in a phantom and cadaver study. Skeletal Radiol. 2012;41:41-9.
38. Schenk O, Huo Y, Vincken KL, van de Laar MA, Kuper IH, Slump KC, et al. Validation of automatic joint space width measurements in hand radiographs in rheumatoid arthritis. J Med Imaging (Bellingham). 2016;3:044502.
39. Landewé RBM, Connell CA, Bradley JD, Wilkinson B, Gruben D, Strengholt S, et al. Is radiographic progression in modern rheumatoid arthritis trials still a robust outcome? Experience from tofacitinib clinical trials. Arthritis Research & Therapy. 2016;18.
40. Fujiwara K, Fang W, Okino T, Sutherland K, Furusaki A, Sagawa A, et al. Quick and accurate selection of hand images among radiographs from various body parts using deep learning. J Xray Sci Technol. 2020;28:1199-206.

Tables

Table 1. Composition of the phantom

	Mixing ratio (TMA powder: adhesive)	Particle size of TMA powder, μm	TMA incineration temperature, °C
Subchondral bone	1:1.2	107～250	1100
Cancellous bone	1:5	107～251	1100

Table 2. Clinical and laboratory characteristics of patients

	baseline	52nd week
Age, median (range) years	54 (32 - 69)	
Sex, female/male	13 / 2	
Duration of disease, median (range) months	50 (26 - 196)	
Duration of CLDA, median (range) months	15 (12 - 19)	
Swollen joint count, range	0-2	0-3
Tender joint count, range	0-2	0-3
DAS28-ESR, mean (SD)	2.03 (0.55)	1.96 (0.57)

CLDA, clinical low disease activity; DAS28, disease activity score with 28 joints; ESR, erythrocyte sedimentation rate; SD, standard deviation

Table 3. Systematic error and SDDs underwater in phantom assessment

	0.1mm interval	0.01mm interval
Mean error, mm	0.001	-0.037
SD of the differences, mm	0.023	0.028
SDD, mm	0.044	0.055

SD, standard deviation; SDD, smallest detectable difference

Figure Legends

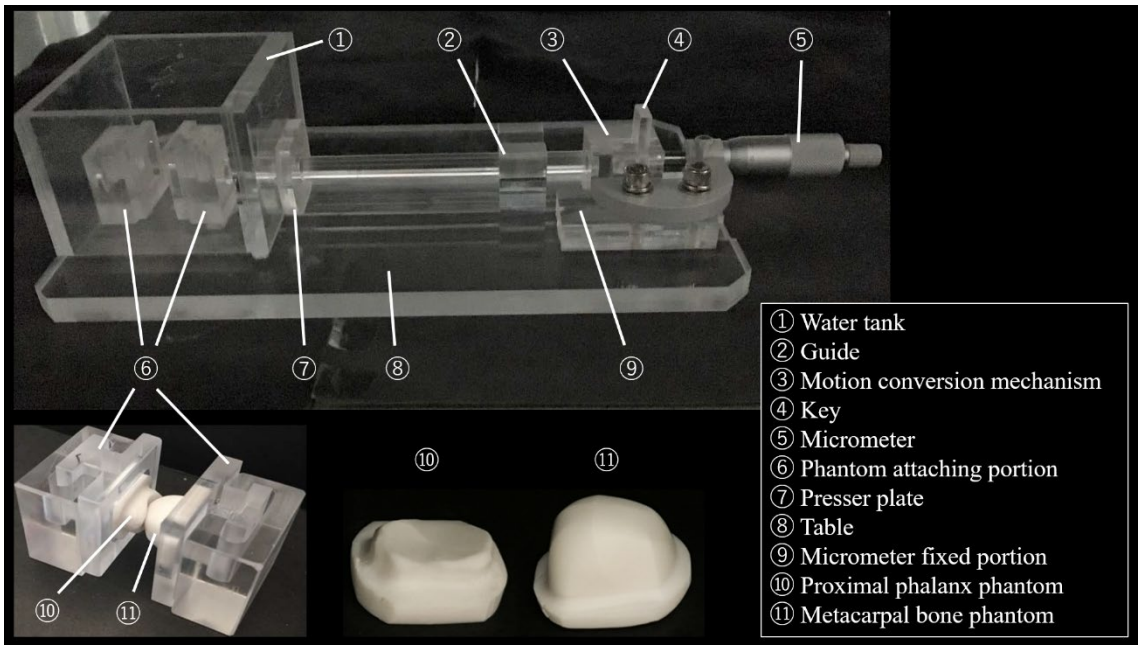

Fig. 1 A metacarpophalangeal joint-shaped two-layer phantom with a water tank

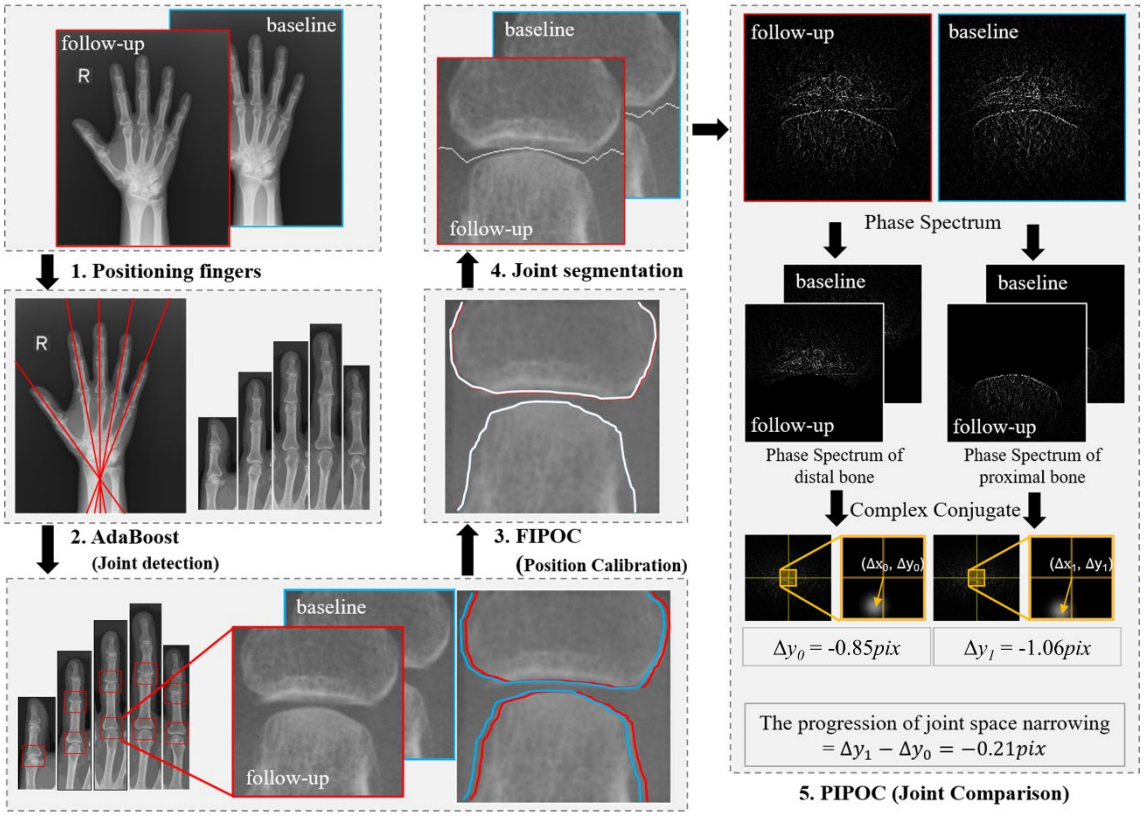

Fig. 2 The algorithm flow of in-house software equipped with PIPOC

FIPOC, full image phase-only correlation; PIPOC, partial image phase-only correlation

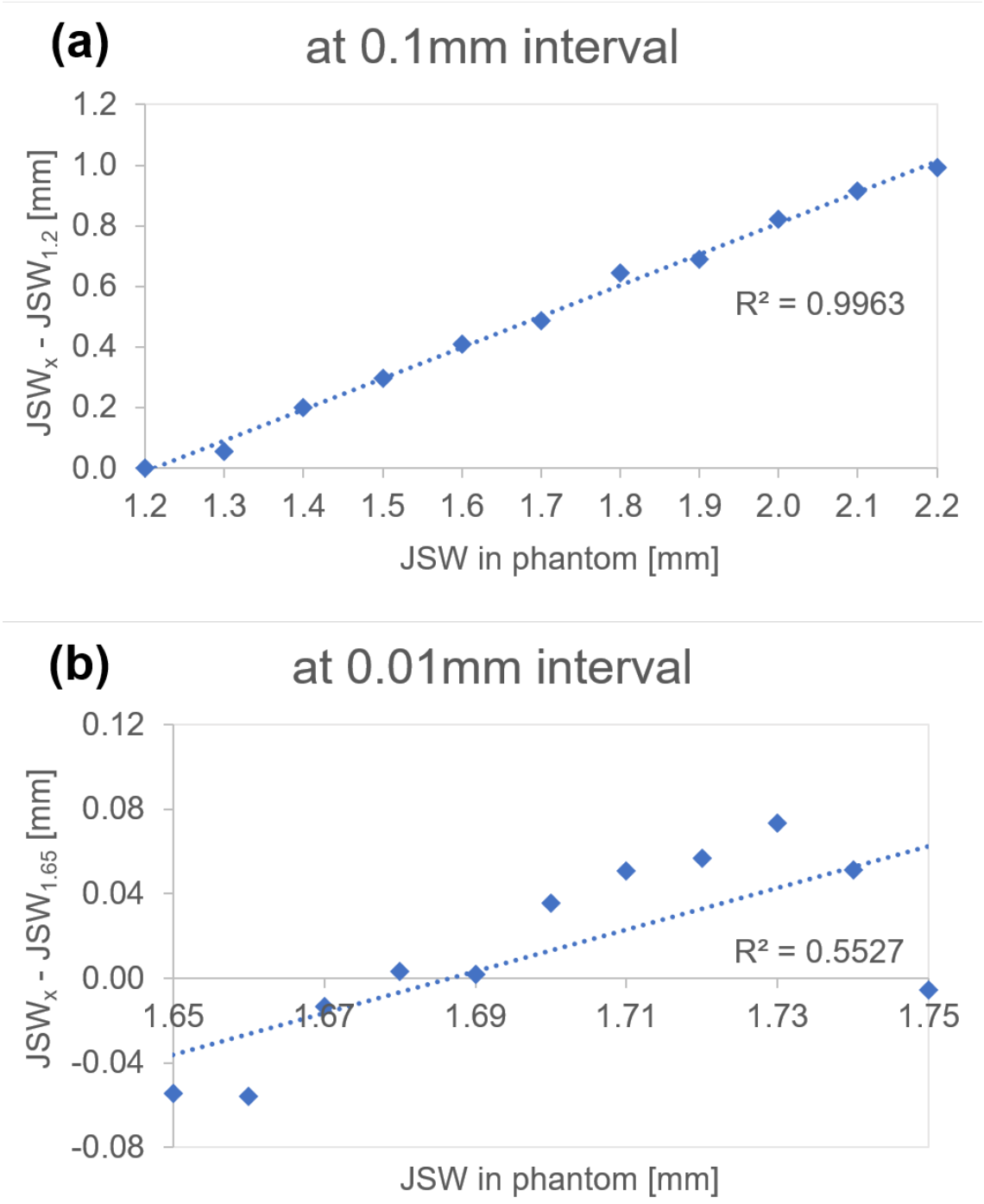

Fig. 3 Correlations between true JSW and measured JSW differences based on 1.2 mm at 0.1 mm (a) and on 1.65 mm at 0.01 mm (b) intervals

JSW, joint space width

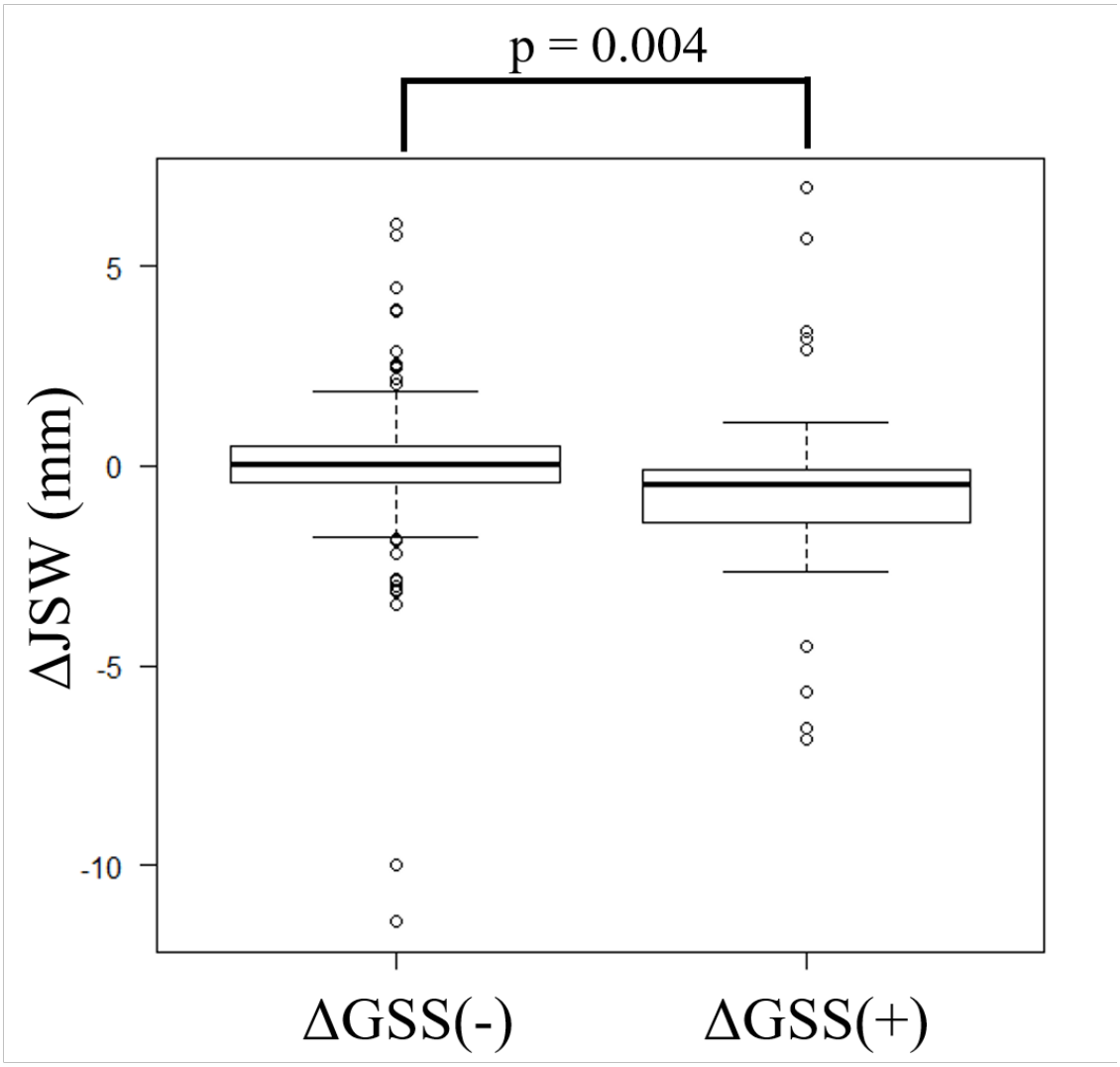

Fig. 4 Comparison of the ΔJSW derived from PIPOC analysis in terms of radiographic JSN progression

JSW, joint space width; GSS, Genant-modified Sharp score; PIPOC, partial image phase-only correlation; JSN, joint space narrowing

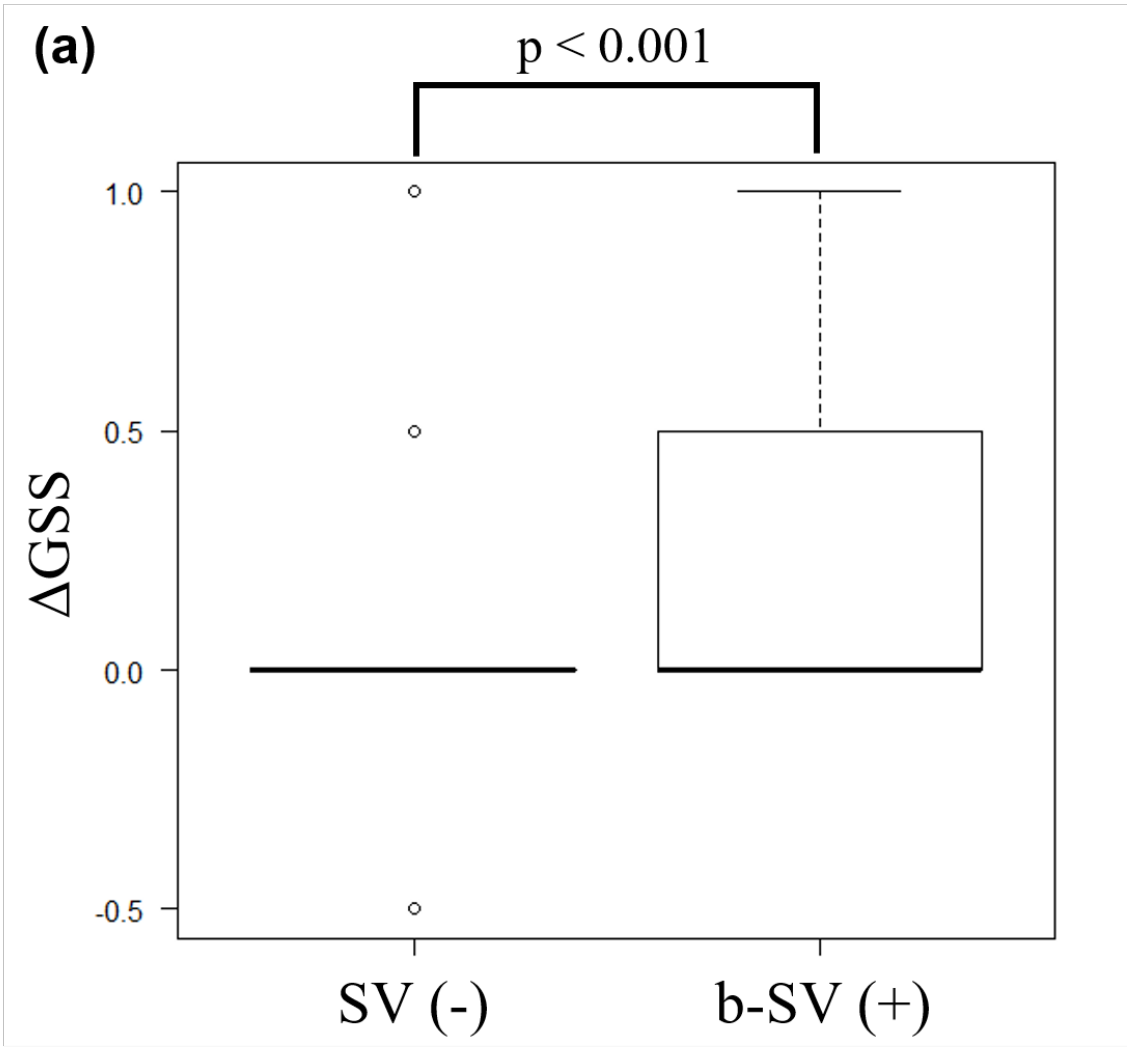
(a)
p < 0.001
1.0
0.5
0.0
-0.5
ΔGSS
SV (-)
b-SV (+)

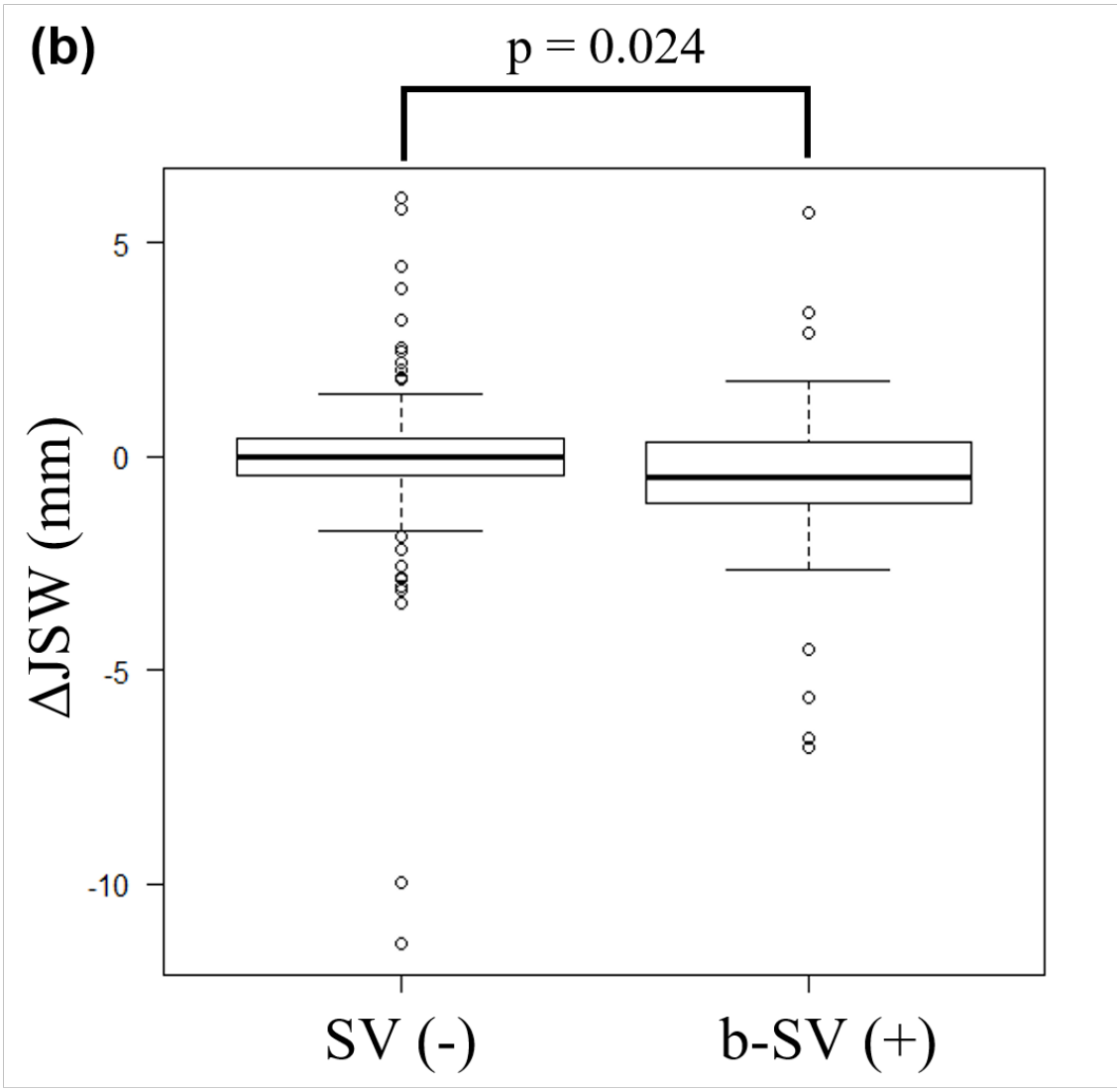

Fig. 5 Comparison of GSS (a) and ΔJSW (b) in terms of baseline SV findings

GSS, Genant-modified Sharp score; JSW, joint space width; SV, synovial vascularity; b-SV, synovial vascularity at baseline

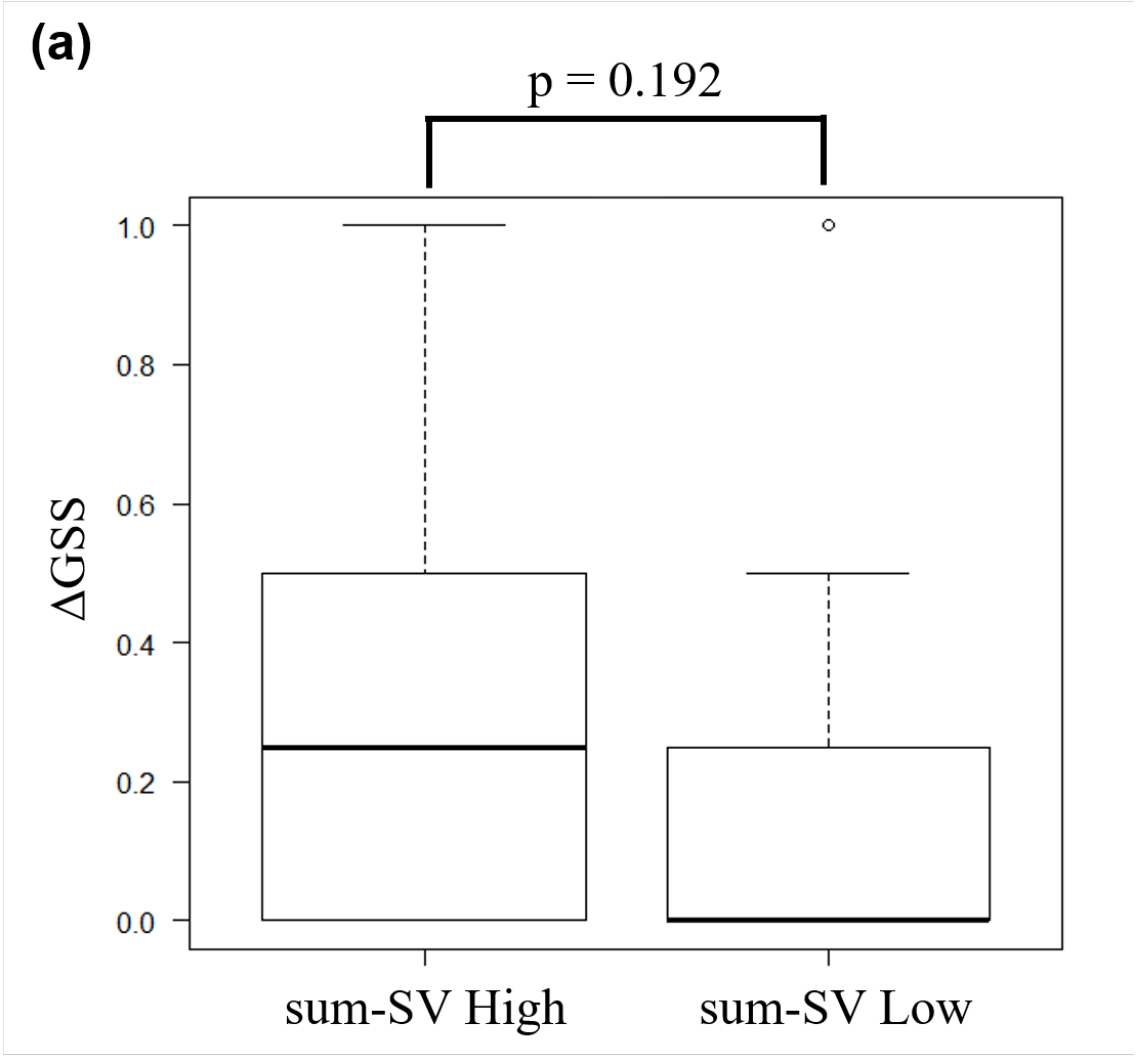
(a)
p = 0.192
1.0
0.8
0.6
0.4
0.2
0.0
ΔGSS
sum-SV High
sum-SV Low

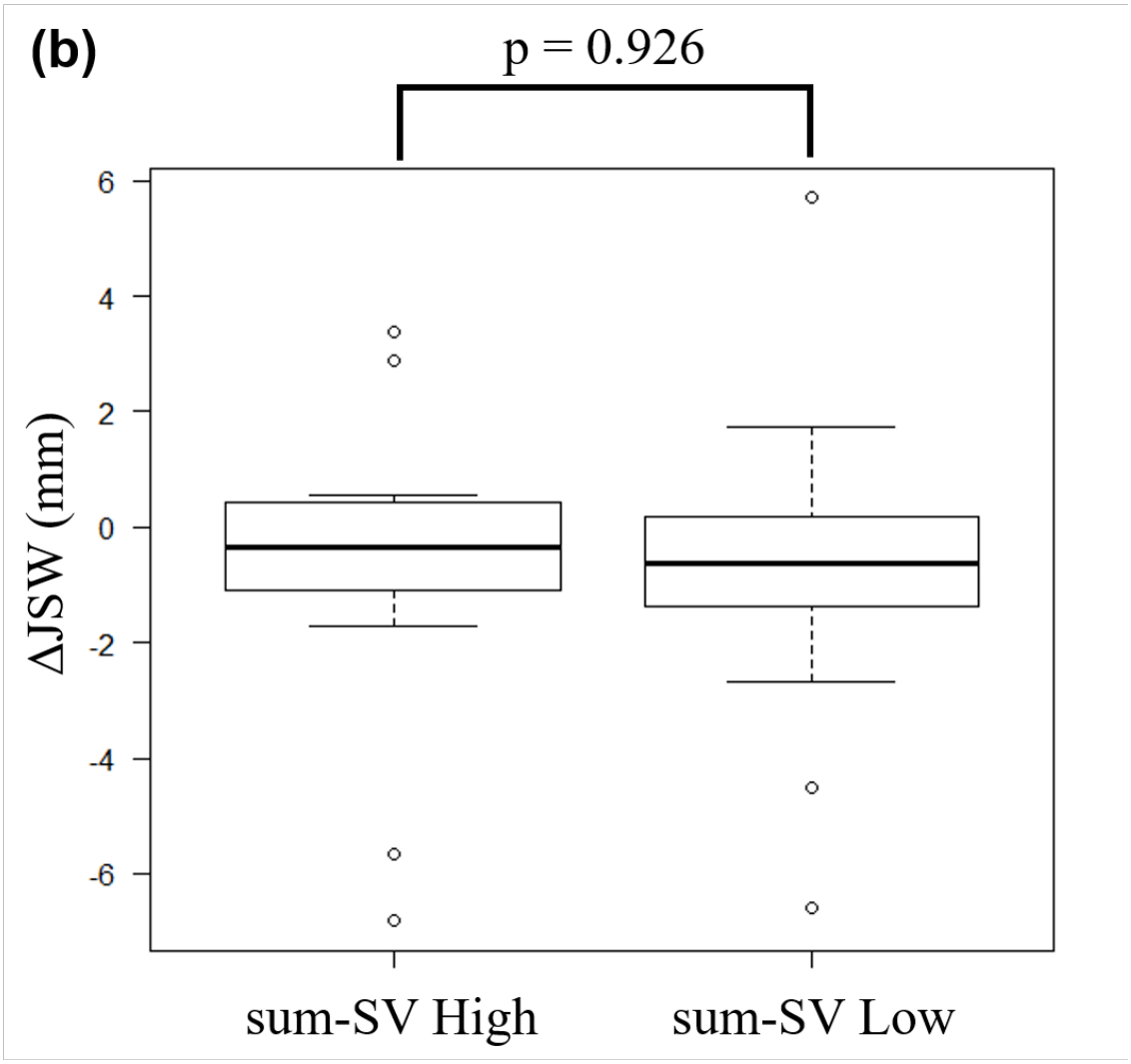

Fig. 6 Comparison of ΔGSS (a) and JSW (b) between the High group and Low group of the sum-SV

GSS, Genant-modified Sharp score; JSW, joint space width; sum-SV, summation of synovial vascularity